



Diethyl sinapate-grafted cellulose nanocrystals as nature-inspired UV filters in cosmetic formulations



D.J. Mendoza^a, M. Maliha^a, V.S. Raghuvanshi^a, C. Browne^a, L.M.M. Mousterde^b,
G.P. Simon^{c,***}, F. Allais^{a,b,**}, G. Garnier^{a,b,*}

^a 15 Alliance Lane (Building 59), Bioresource Processing Research Institute of Australia (BioPRIA), Department of Chemical Engineering, Monash University, Clayton, VIC 3800, Australia

^b URD Agro-Biotechnologies Industrielles (ABI), CEBB, AgroParisTech, 51110, Pomacle, France

^c 14 Alliance Lane (Building 72), Department of Materials Science and Engineering, Monash University, Clayton, VIC 3800, Australia

ARTICLE INFO

Keywords:

Cellulose nanocrystals
Diethyl sinapate
UV-filters
Cosmetics
Cytotoxicity
Antioxidant

ABSTRACT

Inspired by nature's photoprotection mechanisms, we report an effective UV-blocking nanomaterial based on diethyl sinapate-grafted cellulose nanocrystals (CNC-DES). The colloidal stability and UV-blocking performance of CNC-DES in aqueous glycerol (a common humectant in petroleum-free cosmetic formulations) and in a commercially available moisturizing cream were studied. Grafting the water-insoluble DES onto CNCs renders it dispersible in these water-based formulations, thanks to the excellent water-dispersibility of CNC nanoparticles. Glycerol dispersions containing 0.1 to 1.5 wt% CNC-DES display very high UV-blocking activity owing to the anti-UV DES moieties anchored onto CNCs. A facial cream blended with 1.5 wt% CNC-DES exhibits an SPF of 5.03, which is higher than a commercially available sunscreen with the same active ingredient concentration (SPF = 3.84). DPPH radical scavenging assay also showed the antioxidant potential of CNC-DES, albeit coinciding with a significant reduction in antioxidant activity after grafting DES onto CNCs. Cytotoxicity measurements revealed the CNC-DES not to cause significant cytotoxicity to murine fibroblast cells after 24 h of exposure. Overall, CNC-DES exhibits strong anti-UV and antioxidant properties and is water-dispersible, biocompatible, non-greasy, and lightweight. This study demonstrates the exceptional potential of DES-grafted CNCs as nature-inspired UV filters in the next generation of cosmetic formulations, including those for sensitive skins.

1. Introduction

Ultraviolet (UV) light from the sun is necessary for basic life functions and plays an important role in the environment [1]. However, over-exposure to UV radiation can cause many pathological problems in humans, including skin cancer, regarded as the most common type of cancer worldwide [2]. The high energy emanating from UVB radiation (290–320 nm) is primarily responsible for most sunburns and cataracts [3]. On the other hand, UVA radiation (320–400 nm) can induce free radical generation and cause damage to the DNA, proteins, and lipids [4]. Over the years, different sunscreen formulations have been developed to address these issues. Among these are physical sunscreens that usually contain zinc oxide and titanium dioxide and work based on UV reflection mechanism [5]. Physical sunscreens are highly efficient, albeit having

concerns about skin comfort, especially on dry and sensitive skins. Chemical sunscreens, on the other hand, contain synthetic organic compounds such as oxybenzone, octinoxate, octisalate, and avobenzone. These compounds absorb UV and release the energy in the form of heat [6]. However, the long-time use of these chemical sunscreens is associated with unexpected side effects on skins [7]. Therefore, natural UV-absorbing compounds have been sought as a replacement to these concerning chemical sunscreen additives. Ideally, UV filters in sunscreen formulations should exhibit strong anti-UV properties and be water-dispersible, non-greasy, lightweight (easily spreadable and absorb into the skin quickly), non-irradiative, and non-cytotoxic [8].

In nature, plants synthesize UV-absorbing molecules as part of their photoprotection mechanism. Brassicaceous plants, for example, produce sinapate derivatives *via* the phenylpropanoid pathway to protect their

* Corresponding author.

** Corresponding author.

*** Corresponding author.

E-mail addresses: george.simon@monash.edu (G.P. Simon), florent.allais@agroparistech.fr (F. Allais), gil.garnier@monash.edu (G. Garnier).

<https://doi.org/10.1016/j.mtbio.2021.100126>

Received 7 July 2021; Received in revised form 3 August 2021; Accepted 6 August 2021

Available online 18 August 2021

2590-0064/© 2021 The Author(s). Published by Elsevier Ltd. This is an open access article under the CC BY-NC-ND license (<http://creativecommons.org/licenses/by-nc-nd/4.0/>).

leaves against the deleterious effects of UVB radiation [9]. Indeed, these naturally occurring sinapate derivatives have been reported as promising precursors of UV filters that offer exceptional photoprotection, as well as other bioactivities [9–12]. Recently, Horbury et al. [10] reported a novel and nature-inspired sinapate ester, diethyl 2-(4-hydroxy-3,5-dimethoxybenzylidene)malonate or diethyl sinapate (DES). Similar to the naturally occurring sinapate esters, DES displays a strong anti-UV activity (especially in the UVA region) and high photostability. DES can be synthesized using a green Knoevenagel-Doebner condensation [13] reaction of syringaldehyde and diethyl malonate. Its structure contains two identical ethyl ester groups across the acrylic double bond to overcome the classical issues associated with the *cis*- and *trans*-isomer conundrum in sinapate monoesters. Further, DES was reported to exhibit strong antioxidant potential and is not an endocrine-disrupting molecule [10]. The work presented here further highlights the exceptional promise of DES as a UV filter in sunscreen formulations.

Recently, we reported a new and innovative synthetic route to graft phenolic esters on cellulose nanocrystals (CNCs) [14]. We grafted a family of *p*-hydroxycinnamate esters (including DES) on CNCs via a click-type Cu(I)-catalyzed azide-alkyne cycloaddition (CuAAC) [15,16] reaction and reported that the resulting click products display strong anti-UV activity and photostability. The novel phenolic esters and their CNC derivatives are obtained from naturally occurring precursors and prepared via green chemistry methods. Our previous study also showed the important role of the CNC component as an effective dispersing medium for these non-polar phenolic ester derivatives in water and other hydrophilic systems [14,17]. For instance, we showed that grafting diethyl ferulate (DEF) on CNCs allows the efficient dispersion of the phenolic ester in polyvinyl alcohol (PVA) films [17]. Not only did CNCs act as an effective dispersing medium for DEF, but they also served as excellent nano-reinforcements in PVA films. CNCs (or nanocellulose, in general) are ideal nanomaterials for functionalization owing to their tunable surface chemistry, excellent mechanical properties, unique optical properties, and biodegradability [18–20].

Inspired by these findings, we envision that CNCs grafted with DES moieties (CNC-DES) could be ideal UV filters in cosmetic sunscreen formulations as they are sustainable, biofriendly, and effective. In this study, DES is grafted onto CNCs using the same click chemistry approach and rigorously characterized to confirm and quantify the extent of grafting. CNC-DES is incorporated in aqueous glycerol (a common humectant in oil-free cosmetic formulations) and combined with a commercial moisturizing cream. We investigated the colloidal stability of CNC-DES in these media and found that grafting DES onto CNCs increases their dispersibility in these aqueous media. We also show that CNC-DES incorporated in aqueous glycerol and cream exhibits strong anti-UV properties. This study also highlights the antioxidant potential of CNC-DES as measured by 2,2-diphenyl-1-picrylhydrazyl (DPPH) assay. This study explores the potential of CNC-DES as a nature-inspired and highly efficient, sustainable UV filter in cosmetic sunscreen formulations. As part of this, we evaluate the *in vitro* cytotoxicity of CNC-DES using an MTS cell proliferation assay.

2. Experimental

2.1. Materials

All chemicals were analytical grade and used without further purification. Sulfuric acid-hydrolyzed CNCs (98% freeze-dried powder, 0.8–0.9% S) were purchased from the University of Maine, USA. Ascorbic acid, butylated hydroxyanisole (BHA), copper (II) bromide (CuBr₂), dimethylformamide (DMF), glycerol, proline, potassium carbonate (K₂CO₃), *p*-toluenesulfonyl chloride, sodium azide (NaN₃), triethylamine, 6-hydroxy-2,5,7,8-tetramethylchroman-2-carboxylic acid (Trolox), and syringaldehyde were purchased from Sigma-Aldrich. Propargyl bromide (80 wt% in toluene) was acquired from Acros Organics, and diethyl malonate and pyridine were from Tokyo Chemical Industries

(TCI). 2,2-diphenyl-1-picrylhydrazyl (DPPH) radical was acquired from Bio-Strategy Pty Ltd, Australia. Dulbecco's Modified Eagle Medium (DMEM) was purchased from Gibco™, and CellTiter 96® MTS reagent was purchased from Promega, Australia. Cream N (Neutrogena® Oil-Free Moisture) and Cream S (Neutrogena® Oil-Free Moisture Sun Protection Factor (SPF) 15,13.5% active ingredients) are commercially available facial creams purchased in a local pharmacy. DES was synthesized via proline-mediated Knoevenagel condensation of syringaldehyde and diethyl malonate (Figure S1), as we have reported previously [14].

2.2. Synthesis of alkyne-modified DES

Alkyne-modified DES was synthesized via Williamson etherification with propargyl bromide (Figure S2) as reported previously [14,21]. Basically, DES (1 eq, 4.41 g) was initially dissolved in 90 mL anhydrous DMF and cooled to 0 °C. K₂CO₃ (1 eq, 1.89 g) was then added to the reaction mixture, followed by the slow addition of propargyl bromide (1.2 eq, 1.8 mL). The reaction was kept at 0 °C for 30 min and was stirred at room temperature for 16 h under N₂. The reaction mixture was poured into 400 mL of iced water and stirred for 10 min. The final product was isolated by vacuum filtration in a 95% yield. The ¹H and ¹³C NMR spectra of the alkyne-modified DES in (CD₃)₂CO were generated using a Fourier 300 Bruker at 300 MHz (residual signal at δ = 2.05 ppm) and 75 MHz (residual signal at δ = 206.26 and 29.84 ppm) at 20 °C, respectively. The spectra and assignments are given in Figure S3-S4.

2.3. Synthesis of CNC-DES

Azide-grafted CNCs (CNC-N₃) were initially synthesized by tosylation of CNC with *p*-toluenesulfonyl chloride at room temperature for 48 h followed by azidation with NaN₃ at 100 °C for 24 h (Figure S5). DES was then grafted onto CNCs via a click-type Cu(I)-catalyzed azide-alkyne cycloaddition reaction between CNC-N₃ and alkyne-modified DES (DES-PB) as previously described [14,17] (Figure S6). CNC-N₃ (1 eq, 1 g) and DES-PB (1 eq, 1 g) were suspended in 100 mL DMF. A 10 mL DMF solution containing CuBr₂ (0.14 g), ascorbic acid (0.4 g), and triethylamine (1 mL) was slowly added, and the reaction was allowed to proceed at 60 °C for 24 h. The click product was isolated by precipitation with 500 mL ethanol, followed by repeated centrifugation at 11,000 rpm for 20 min and washing with ethanol and water. The CNCs were purified by dialysis against Milli-Q water for 10 days using a cellulose dialysis membrane (MW cut-off 12,000–14,000). Powdered CNC-DES was obtained in a 54% yield (1.08 g) after freeze-drying for 48 h.

2.4. Incorporation of CNC-DES in glycerol and cream

An aqueous CNC-DES suspension (2 wt%) was initially prepared by suspending a known amount of the freeze-dried CNC-DES in water followed by ultrasonication (Sonics VCX 750) for 5 min at 19.5 kHz, 750 Watts, and 70% amplitude (ON/OFF, 5 s). The stock aqueous CNC-DES suspension was further diluted with 10 wt% glycerol to prepare 0.1–1.5 wt% glycerol dispersions. Similarly, the glycerol dispersions were ultrasonicated using the same conditions. Creams loaded with 0.1–1.5 wt% CNC-DES were also prepared by combining Cream N and designated amounts of aqueous CNC-DES and stirring overnight.

2.5. Characterization

2.5.1. Elemental analysis

The amount of carbon, nitrogen, oxygen, and sulfur in the CNC derivatives was quantified using a Thermo Scientific FlashSmart CHNS elemental analyser. The degree of substitution (DS) of CNC-N₃ was directly calculated from the %N while the DS of CNC-DES was quantified from %C and calculated using (1) as previously reported [22]:

$$DS = \frac{6 \times M_C - \%C \times M_{AGU}}{M_g \times \%C - M_{Cg}} \quad (1)$$

where $6 \times M_C$ is the carbon mass of one anhydroglucose unit (72.07 g/mol), M_{AGU} is the mass of anhydroglucose unit (162.14 g/mol), M_g is the mass of the grafted moiety (404.4 g/mol), and M_{Cg} is the carbon mass of the grafted moiety (228.19 g/mol).

The degrees of surface substitution (DS_{surf}) were also derived from the DS values using (2):

$$DS_{surf} = DS/R_c \quad (2)$$

where R_c is the CNC chain ratio = 0.29 [23].

2.5.2. X-ray photoelectron spectroscopy (XPS)

The surface chemical composition of the CNCs was characterized using a Thermo Scientific Nexsa XPS spectrometer equipped with an Al K α irradiation source. Elemental survey scans were recorded from -10 to 1350 eV with a scan step of 1 eV. High-resolution N 1s and C 1s analyses were also performed in the range of 392–410 eV and 279–298 eV, respectively. Thermo Scientific Avantage software was used for all data processing and peak deconvolution.

2.5.3. Fourier transform infrared (FTIR) spectroscopy

The FTIR spectra of pristine CNC and CNC-derivatives were recorded using attenuated total reflectance (ATR)-FTIR spectrometer (Agilent Technologies Cary 630). The spectra were generated at 4 cm⁻¹ resolution with 32 scans in the range of 4000–500 cm⁻¹.

2.5.4. ICP-OES

The amount of copper in CNC-DES was quantified using a PerkinElmer Avio 200 Inductively Coupled Plasma-Optical Emission Spectrometer (ICP-OES) as reported previously [24,25]. A known amount of CNC-DES was loaded in tared crucibles and ashed in a muffle furnace operating at 600 °C for 3 h. The resulting ash was then digested in concentrated nitric acid and diluted with 3% nitric acid.

2.5.5. Zeta potential

The zeta potential of 0.1 wt% CNC and CNC-DES dispersed in 10% glycerol was measured using a Brookhaven Nanobrook Omni particle analyzer. Measurements were performed in five replicates per sample, and the average and standard deviations are reported.

2.5.6. UV-vis spectroscopy and in-vitro SPF quantification

All UV-vis transmission scans were recorded in a Cary60 UV-vis spectrophotometer (Agilent Technologies). Glycerol dispersions of CNC-DES were loaded in quartz cuvettes, and the transmission scans were generated from 200 to 800 nm in a 1 nm resolution.

The SPF values of the creams were measured *in vitro* using a previously reported method [26]. In brief, the creams (2 mg/cm²) were applied on a 3 M Transpore® tape (2 layers, 19 mm × 35 mm) attached on a quartz slide. The slide with the creams was then placed in the dark and dried for 20 min prior to UV-vis measurement. Transmission scans of the slides were recorded in the range of 290–400 nm in a 1 nm resolution. The transmittance scans of the samples were corrected by subtracting the transmittance scans of the slide and tape. For comparison, the transmittance scans of Cream S were also measured. Note that Cream S with an active ingredient concentration of 1.5 wt% was also prepared by diluting the original formulation (13.5 wt%) with 10 wt% glycerol. The SPF was calculated using a modified Mansur equation [27] (3):

$$SPF_{in\ vitro} = \frac{\sum_{290}^{400} E_{\lambda} S_{\lambda}}{\sum_{290}^{400} E_{\lambda} S_{\lambda} T_{\lambda}} \quad (3)$$

where E_{λ} is the erythemal spectral effectiveness, S_{λ} is the solar spectral irradiance, and T_{λ} is the %transmittance of the sample.

2.5.7. Transmission electron microscopy (TEM)

The morphology and size distribution of CNC particles were analyzed using an FEI Tecnai F20 transmission electron microscope. The CNC dispersions were diluted to ~0.001 wt%, dried on plasma-cleaned copper grids, and stained with 2% uranyl acetate. TEM micrographs were generated at 200 kV.

2.6. Evaluation of antioxidant potential by DPPH radical scavenging activity

The measurement of DPPH radical scavenging activity of CNC-DES was adapted from methods reported previously [10,28] with some modification. A stock DPPH solution (200 μM) was prepared by dissolving a known amount of DPPH in ethanol. In a 96-well plate, 150 μL of DPPH was added to 50 μL of CNC-DES glycerol dispersions at different concentrations (0.1–1.5 wt%). The mixture was then incubated in the dark at room temperature for 1 h, and the absorbance at 517 nm was measured using a microplate reader (Tecan Infinite M Nano). For comparison, varying concentrations of DES, alkyne-modified DES, pristine CNC, and some antioxidant standards (ascorbic acid, Trolox, and BHA) were also tested. The absorbance of DPPH solution without the samples (blank) was also measured. The DPPH radical scavenging activity was calculated using 4:

$$DPPH\ Radical\ Scavenging\ Activity\ (\%) = \frac{A_0 - A_1}{A_0} \times 100 \quad (4)$$

where A_0 is the absorbance of the blank at 517 nm and A_1 is the absorbance of the DPPH solution with the samples at 517 nm.

The % scavenging activity was plotted against sample concentration and the efficient concentration needed to scavenge DPPH radicals by 50% (EC_{50}) was calculated from the plot.

2.7. Evaluation of cytotoxicity

Murine fibroblast cell line L929 was cultured in DMEM supplemented with 10% (v/v) fetal bovine serum (FBS) and 1% penicillin and streptomycin. Stock CNC-DES dispersions (6, 4, 2, and 0.4 wt%) were diluted in the culture medium to achieve treatment concentrations of 1.5, 1, 0.5, and 0.1 wt%. DMEM containing 1.5 wt% pristine CNC and 10% glycerol was also tested. The 96-well plates were seeded with 10,000 cells/well and incubated at 37 °C and 5% CO₂ for 24 h to allow attachment to the tissue culture polystyrene (TCPS). The media was aspirated, the cells were washed with PBS, and the treatment media were added to the wells. The positive and negative controls were treated with 10% (v/v) dimethyl sulfoxide (DMSO) and fresh DMEM, respectively. After 24 h of incubation, the treatment media was replaced with an MTS reagent and incubated for 1 h in the dark. The absorbance at 490 nm was read using a Thermo Scientific Multiskan Spectrum multiplate reader. The experiment was performed in three technical replicates with independent biological triplicates. The percentage viability was computed by normalizing the absorbance with respect to the negative control (untreated cells). The cells were also observed under an optical microscope (Nikon Eclipse Ts2) to investigate the changes in the morphology of the cells.

Statistical analysis of the results from the biological triplicates was performed using GraphPad Prism 8.0.2 by one-way analysis of variance (ANOVA), with significance assigned at $p < 0.05$, followed by Tukey's post hoc test to compare individual pairs of data.

3. Results

3.1. Synthesis of diethyl sinapate-grafted CNCs

Grafting of diethyl sinapate onto cellulose nanocrystals was achieved via a Cu(I)-catalyzed cycloaddition reaction between azide-modified CNCs (CNC-N₃) and alkyne-bearing diethyl sinapate (DES) (Figure S6).

Successful anchoring of DES moieties on CNC surface was supported by a combination of analyses (FTIR, XPS, TEM) shown in Figure S7. FTIR revealed the conversion of azide to triazole groups as evidenced by the 57% decrease in peak intensity at 2110 cm^{-1} for the antisymmetric azide stretching motion [29]. High-resolution N 1s analysis from XPS also showed that CNC-DES exhibits a single, sharp peak at 401 eV, confirming the conversion of the azide group into a 1H-1,2,3-triazole ring triazole ring [30]. Further, high-resolution C 1s analysis revealed the appearance of a new peak at 289 eV assigned to carboxylic groups (O-C=O) attributed to the presence of ester groups in DES grafted on CNCs [22]. Grafting of DES on CNCs afforded a DS_{surf} of 0.28, corresponding to 56% conversion of the azide groups to triazole ring. TEM also revealed that the CNCs retained their rod-like and nanosized morphology after the click reaction. These results confirm that the click reaction employed is highly efficient, similar to the results we have previously reported [14,17].

3.2. UV-blocking property of CNC-DES in glycerol and cream

CNC-DES was dispersed in 10 wt% glycerol to mimic common, petroleum, and oil-free cosmetic formulations where glycerol is used as a humectant for water-based formulations. Figure S8 shows that aqueous dispersions of CNC and CNC-DES can be dispersed in 10% glycerol via ultrasonication. Pristine CNCs and functionalized CNC-DES in glycerol exhibited zeta potentials of $-57.13 \pm 0.94\text{ mV}$ and $-49 \pm 1.29\text{ mV}$, respectively. On the contrary, DES is not dispersible or soluble in 10% glycerol due to its hydrophobic structure. This shows that grafting DES onto CNCs rendered it dispersible in aqueous glycerol and that CNC served as an effective dispersing medium for the non-polar phenolic ester. Fig. 1a shows that CNC-DES dispersed in aqueous glycerol solutions exhibits a very high UV-blocking performance. At 285 and 325 nm, the % transmittance of the CNC-DES suspension abruptly decreased after the addition of 0.1% CNC-DES (Fig. 1b). At concentrations $\geq 0.5\text{ wt\%}$, zero transmittance of UVA, UVB, and UVC was measured. On the other hand, pristine CNCs do not exhibit any appreciable UV blocking properties at 0.1–1.5 wt% (Figure S9). Fig. 1c also shows that the incorporation of CNC-DES imparts a deep yellowish color to the glycerol solution. This is

attributed to the presence of residual copper in CNC-DES during the click reaction.

The *in vitro* SPF of creams blended with CNC-DES was quantified. Similar to glycerol, ultrasonicated, aqueous CNC-DES can be dispersed in the cream by overnight stirring with a magnetic stirrer. The blending of DES with the cream resulted in an aggregation of DES particles suggesting that DES is not colloiddally stable in the cream. Fig. 2a shows the transmittance spectra of Cream N blended with different concentrations of CNC-DES. As expected, Cream N does not exhibit any appreciable UV-shielding property by itself, as evidenced by the 90–100% transmission of UV light. However, after the addition of CNC-DES in Cream N, the UV blocking properties improved dramatically. Low to moderate transmission of UV light was measured depending on the concentration of CNC-DES added. On the other hand, the commercially available sunscreen formulation, Cream S, exhibits a stronger and broader wavelength UV protection. This is expected because of the presence of UV filtering compounds in Cream S such as avobenzone, octinoxate, octisalate, octocrylene, and oxybenzone that strongly absorb in the UVA and UVB regions. Interestingly, at the same active ingredient concentration (1.5 wt %), CNC-DES displays a comparable UV protection relative to Cream S.

Using the Mansur equation (Eq. (3)), the SPF of the creams was quantified (Table 1). Cream S exhibited an SPF of 15.2, in agreement with the product SPF label. The SPF of Cream N blended with CNC-DES increases with increasing CNC-DES concentration. However, the addition of pristine CNC did not cause any significant improvement in the SPF of Cream N. This shows that the increase in SPF of these creams can be attributed to the DES moieties grafted onto CNCs. Interestingly, at the same active ingredient concentration, Cream N blended with 1.5 wt% CNC-DES has a higher SPF than the commercial sunscreen, Cream S (SPF 5.03 vs 3.84).

3.3. Antioxidant potential of CNC-DES

The antioxidant potential of CNC-DES was evaluated by DPPH radical scavenging assay. The assay is based on the ability of potential antioxidants to donate a hydrogen atom to a DPPH radical. Upon hydrogen

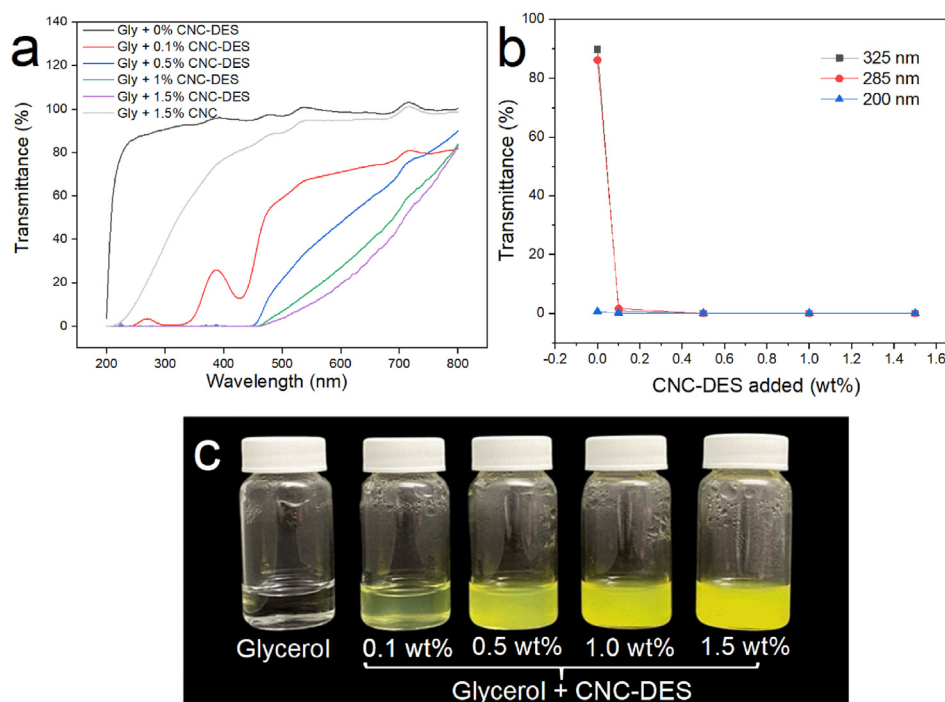


Fig. 1. UV-blocking property of glycerol dispersions as a function of CNC-DES concentration. (a) UV-Vis transmittance spectra of 10% glycerol, 1.5 wt% pristine CNCs in 10% glycerol, and varying concentrations (0.1–1.5 wt%) of CNC-DES in 10% glycerol. (b) Effect of CNC-DES concentration on the optical transmittance at different UV wavelengths. (c) Photographs of CNC-DES-glycerol dispersions at different concentrations.

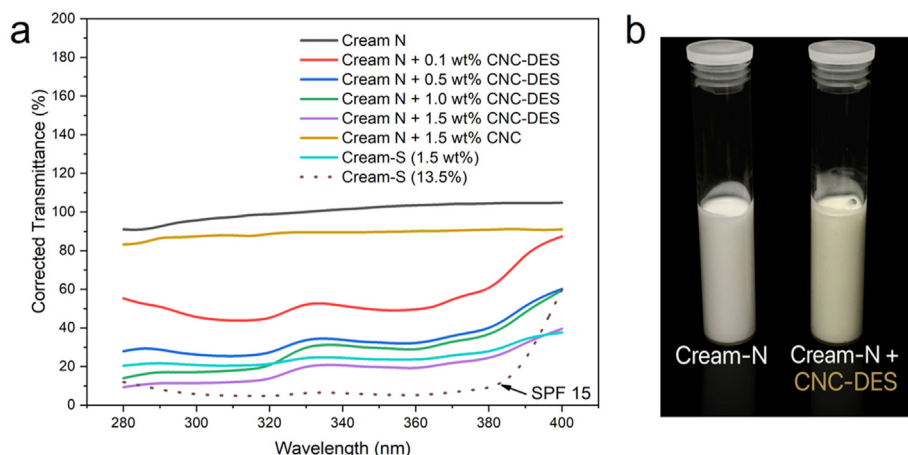


Fig. 2. UV blocking property of CNC-DES blended in Cream N. (a) UV transmittance spectra of Cream N, Cream N blended with varying concentrations (0.1–1.5 wt%) of CNC-DES, and Cream S (1.5–13.5 wt% active ingredients). (b) Photographs of Cream N and Cream N + CNC-DES formulations.

Table 1

SPF of Cream N, Cream N blended with varying concentrations (0.1–1.5 wt%) of CNC-DES, and Cream S (1.5–13.5 wt% active ingredients).

Sample	SPF
Cream N	0.96 ± 0.14
Cream N + 0.1 wt% CNC-DES	2.22 ± 0.28
Cream N + 0.5 wt% CNC-DES	2.82 ± 0.50
Cream N + 1.0 wt% CNC-DES	3.64 ± 0.08
Cream N + 1.5 wt% CNC-DES	5.03 ± 0.71
Cream N + 1.5 wt% CNC	1.10 ± 0.05
Cream S (1.5 wt% of UV filters)	3.84 ± 0.65
Cream S (13.5 wt% of UV filters)	15.20 ± 2.84

acceptance, the DPPH radical is reduced to its corresponding hydrazine, resulting in a concomitant loss of its original violet color [31]. The radical scavenging activity of the antioxidant standards, DES, alkyne-modified DES, pristine CNC, and CNC-DES are presented in Fig. 3. In line with expectation, the commercial antioxidant standards, ascorbic acid, Trolox, and BHA, exhibit moderate to high scavenging activities depending on the concentration. These standards exhibited more than 80–90% scavenging of DPPH radical at 400 μM concentration. At the same concentration, DES and alkyne-modified DES exhibit lower scavenging activities relative to the standards. Even at elevated concentrations ($\geq 400 \mu\text{M}$), DES could only scavenge at most 65% of the original amount of DPPH radical. Interestingly, the scavenging activity of DES dramatically decreased after the addition of an alkyne moiety (at most 25% scavenging activity).

Using the same range of concentration as in the SPF experiments, the DPPH radical scavenging activities of CNC-DES was quantified (Fig. 3b). For comparison, the scavenging activity of CNC was also tested. As expected, pristine CNCs exhibited a very low to moderate scavenging ability. The activity that does exist can arise from the presence of residual lignins [26] in CNC and the reducing end groups (aldehydes) [32] present in cellulose. After grafting of DES, the scavenging activities of CNC improved by 2- to 6-folds, depending on the concentration. The apparent antioxidant properties of CNC-DES can be attributed to the synergistic antioxidant properties of CNC and DES, as shown by our results.

Table 2 presents the EC_{50} values of the standards, DES, alkyne-modified DES, pristine CNC, and CNC-DES. The EC_{50} corresponds to the minimum concentration of the material at which 50% of the DPPH radicals have been reduced. This value is a measure of the antioxidant potential of a material with the lower the EC_{50} , the stronger being the antioxidant potential. Apparently, these values could not be detected in the case of alkyne modified DES and pristine CNC, even at higher

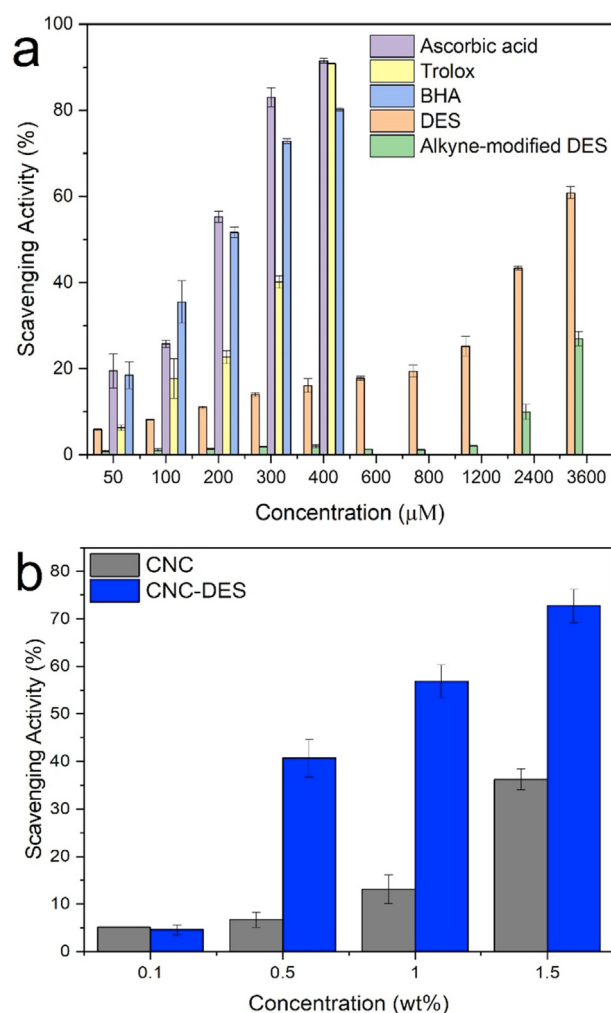


Fig. 3. DPPH radical scavenging activity of antioxidant standards, DES, and alkyne-modified DES (a). DPPH radical scavenging activity of pristine CNC and CNC-DES at different concentrations (0.1–1.5 wt%) (b).

concentrations. Relative to the standards, DES has 16–30x higher EC_{50} (927.02 $\mu\text{g}/\text{mL}$). This supports the study of Horbury et al. [10] where a lower antioxidant activity of DES was observed compared to Trolox, BHT, and BHA. CNC-DES, on the other hand, has an EC_{50} of 8658.28 $\mu\text{g}/\text{mL}$,

Table 2

EC₅₀ of antioxidant standards, DES, and alkyne-modified DES, pristine CNC, and CNC-DES against DPPH radical.

Sample	EC ₅₀ (μg/mL)
Ascorbic acid	31.38
Trolox	55.82
BHA	32.35
DES	927.02
Alkyne-modified DES	Not detected
CNC	Not detected
CNC-DES	8658.28

which suggests that the antioxidant potential of CNC-DES is inferior to that of the standards and DES.

3.4. Cytotoxicity of CNC-DES

The cytotoxic effect of CNC-DES and CNC was investigated *in-vitro* on murine fibroblast cell lines (Fig. 4). Cells treated with the negative control (Fig. 4a) show a confluent layer of healthy fibroblasts. In contrast, cells treated with 10% DMSO (Fig. 4b) were rounded and detached from the surface of the plate, suggesting that these cells are non-viable. Importantly, cells exposed to glycerol, pristine CNC, or CNC-DES (Fig. 4c–f) also appear to be viable, as similar to the negative control. The cell viability after exposure to CNC-DES was quantified using the MTS assay (Fig. 4g). These results demonstrate that pristine CNCs did not have a significant effect on the viability of the cells. At the highest concentration of CNC-DES (1.5 wt%), the percentage viability was 82%, which is defined as non-toxic according to the ISO 10993-5 standard [33]. This standard states that any material that leads to a viability less than 70% is cytotoxic. Post-hoc statistical analysis revealed that the viability of cells treated with CNC-DES is not significantly different from that of the untreated cells, regardless of the CNC-DES concentration tested. Hence, CNC-DES is not cytotoxic to murine fibroblast cells.

4. Discussion

In this paper, we have reported the potential of DES-grafted CNCs as UV filters in modern cosmetic formulations. The results show that grafting DES onto CNCs aids in the dispersion of the hydrophobic DES in aqueous glycerol and oil-free moisturizing cream. This can be attributed to the several hydroxyl groups and negatively charged sulfate half-ester groups found in CNCs, which render CNC-DES dispersible in hydrophilic matrices. We have previously demonstrated this effect with a hydrophilic polymer, polyvinyl alcohol (PVA) [17]. A similar effect was also observed by Zhang et al. when cinnamate-grafted CNCs were dispersed in water, PVA, and polystyrene (PS) [34]. Importantly, grafting DES imparted excellent anti-UV properties to CNCs. CNC-DES (≥ 0.5 wt%) dispersed in aqueous glycerol exhibits strong anti-UV properties, blocking the transmission of light in all the UVA, UVB, and UVC regions. It should be noted that at higher concentrations, the reduced transmittance of UV and visible light is due to the scattering of the CNC-DES particles instead of absorbance. When incorporated in an oil-free moisturizing cream, the SPF of CNC-DES is higher than those of the commercial sunscreen at the same active ingredient concentration. The anti-UV properties of CNC-DES can be solely attributed to the DES moieties that are covalently anchored to the CNC surfaces. The CNC-DES is effective in this regard by absorbing the detrimental energy from UV rays to dispersing it to the environment in the form of heat [35]. DES, in particular, can undergo an efficient *trans-cis* and *cis-trans* photoisomerization, resulting in a photo-equilibrium between the isomers [10,36].

DPPH radical scavenging assay reveals that grafting DES on CNCs drastically reduces its antioxidant property. This is most likely due to the etherification of the phenolic group in DES, which is the functionality primarily responsible for the DPPH radical scavenging activity of DES [10]. The free hydroxyl group in phenol and hydroxycinnamate

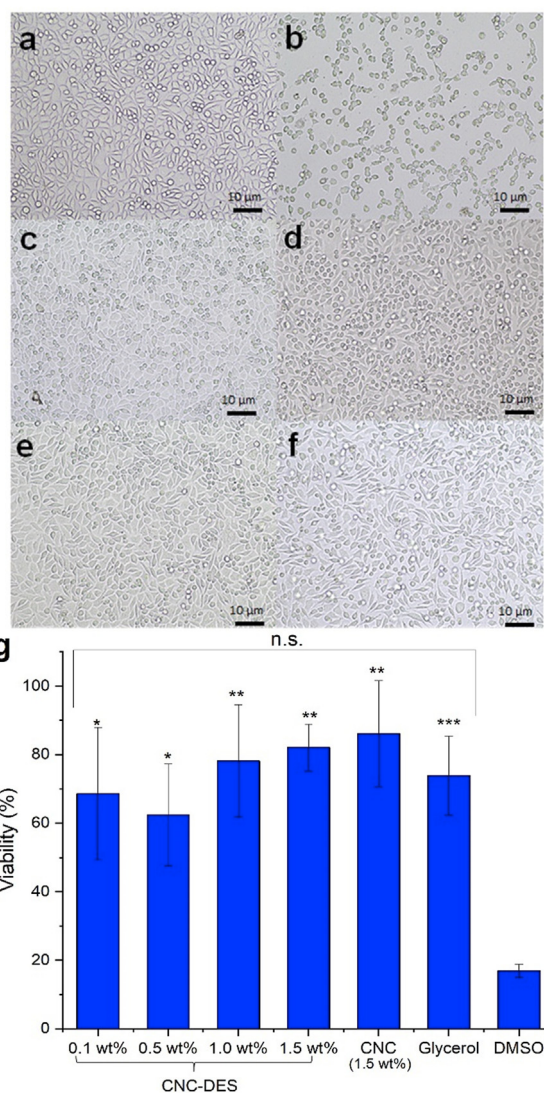


Fig. 4. Cytotoxicity of CNC-DES. Optical light micrographs of L929 cells after 24 h of incubation with DMEM media only (a), 10% DMSO (b), 10% glycerol (c), 1.5 wt% pristine CNC (d), 0.1 wt% CNC-DES (e), and 1.5 wt% CNC-DES (f). Normalized cell viability of L929 cells after 24 h of incubation with varying concentrations of CNC-DES (0.1–1.5 wt%), CNC (1.5 wt%), 10% glycerol, and 10% DMSO. The data are expressed as mean \pm standard deviations for triplicates from three independent sets of biological replicates. All treatments, except DMSO, are not significantly different from DMEM media only (negative control). The number of asterisks over the bars indicates the level of significance of the data as compared with 10% DMSO. * $p \leq 0.05$, ** $p \leq 0.01$, *** $p \leq 0.001$, n.s. – no significant difference (g).

derivatives can donate a hydrogen atom to reduce the DPPH radical to its corresponding hydrazine derivative [37–39]. However, the free hydroxyl group in DES is lost after the click reaction, and therefore, no free hydrogen atoms can be abstracted by the DPPH radical. Interestingly, a previous study reported that cinnamate derivatives could scavenge free radicals through their side acrylic double bond functional groups. Waterhouse et al. [40] proposed that the free radical can attack the α,β -unsaturated side-chain in cinnamate derivatives, attaching at the α carbon to produce a resonance-stabilized benzyl radical. The apparent antioxidant activity of CNC-DES can also be attributed to traces of ascorbic acid that may not have been completely removed after the click reaction. The EC₅₀ of CNC-DES was found to be 8658.28 μg/mL, which is 155- to 268-folds higher than the standards and 9-folds higher than DES. This value is equivalent to 0.83 wt% of CNC-DES. If CNC-DES is added to

the cosmetic formulation above this concentration, a comparable antioxidant property can arise, as with the antioxidant standards. Nevertheless, the addition of any of these commercial antioxidants in cosmetic formulations is beneficial to the skin. The potential antioxidant activity of CNC-DES dispersed in glycerol or cream is beneficial as it contributes to maintaining a healthy skin barrier. Antioxidants can neutralize reactive oxygen species (ROS) induced by UV radiation [41].

MTS assays also reveal that CNC-DES is not cytotoxic to murine fibroblast cells after 24 h of exposure. However, it should be noted that the copper concentration is crucial in CNC-DES cytotoxicity. Our results reveal that the amount of residual copper in CNC-DES significantly influences its cytotoxicity. Indeed, several studies have reported the detrimental effects of copper on biological systems [42–45]. The presence of copper in CNC-DES arises from CuBr₂ that is used as a catalyst in the click reaction. We initially added 140,000 ppm of CuBr₂ to the reaction mixture. After isolation and purification by dialysis for 3 days, the amount of copper retained in CNC-DES was reduced to ~5100 ppm. At this copper concentration, we found that CNC-DES can kill more than 80% of the cells at 1.5 wt% concentration.

To address this problem, CNC-DES was re-dialyzed for an additional 7 days, which further decreased the copper concentration in CNC-DES by 50-folds (102 ppm). Further increase in dialysis (by at least 10 days) could ensure the removal of most copper ions. It is also possible to lower the initial CuBr₂ concentration used in the reaction; however, this effect on the properties of the grafted CNCs requires investigation. The cytotoxicity of CNC-DES may also arise from the presence of the triazole ring, a potential skin irritant; the pathomechanisms involved are poorly understood [46].

Ultimately, this study shows the potential of CNC-DES as a sustainable and performant sunscreen additive able to substitute commercially available chemical UV filters. CNC-DES dispersed in aqueous glycerol exhibits strong UV blocking properties and high visible light transmittance, making it ideal as a non-whitening UV filter in sunscreen formulations. Also, the ability of CNC-DES to be dispersed in glycerol and oil-free moisturizing creams makes it suitable for water-based sunscreen formulations that are typically non-irritant (for sensitive skins), non-greasy, and should have a 'lightweight' feel. The antioxidant potential of CNC-DES is an added benefit to the sunscreen formulation. Importantly, these CNC-based UV filters are not considered cytotoxic to skin cells *in vitro*.

5. Conclusion

In this study, we report a novel and nature-inspired UV filter based on diethyl sinapate-grafted cellulose nanocrystals (CNC-DES) dispersible in aqueous glycerol and water-based cosmetic creams. Grafting the water-insoluble DES onto CNCs renders it dispersible in water and 10% glycerol, while the DES itself is not water-dispersible. Glycerol dispersions containing 0.1–1.5 wt% CNC-DES display very high anti-UV activity. An oil/petroleum-free moisturizing cream blended with 1.5 wt% CNC-DES exhibits an SPF of 5.03, higher than a commercially available sunscreen with the same active ingredient concentration (SPF = 3.84). DPPH radical scavenging assay also shows the antioxidant potential of CNC-DES. Notably, the antioxidant activity of DES dramatically reduces after the click reaction, which is most likely due to the etherification of the phenolic group in DES. *In vitro* MTS cell proliferation assay also reveals that CNC-DES is not cytotoxic to murine fibroblast cells after 24 h of exposure. Overall, CNC-DES possesses strong anti-UV and antioxidant properties and is water-dispersible, biocompatible, non-greasy, and lightweight. This study demonstrates that CNC-DES is a highly promising, nature-inspired UV filter that can be engineered and applied in cosmetic formulations, including for sensitive skins.

Data availability

The raw/processed data required to reproduce these findings cannot be shared at this time as the data also forms part of an ongoing study.

CRediT author statement

David Joram Mendoza: Conceptualization, Methodology, Formal analysis, Investigation, Visualization, Writing - Original Draft, **Maisha Maliha:** Methodology, Investigation, Writing - Original Draft, **Vikram Singh Raghuvanshi:** Investigation, Supervision, **Christine Browne:** Investigation, Supervision, **Louis M.M. Mouterde:** Conceptualization, Supervision, Writing - Review & Editing, **Florent Allais:** Conceptualization, Writing - Review & Editing, Supervision, Funding acquisition, **George P. Simon:** Conceptualization, Supervision, Writing - Review & Editing, **Gil Garnier:** Conceptualization, Writing - Review & Editing, Project administration, Supervision, Funding acquisition.

Declaration of competing interest

The authors declare that they have no known competing financial interests or personal relationships that could have appeared to influence the work reported in this paper.

Acknowledgements

Funding from the Australian Research Council-Industry Transformation Research Hub; Processing Advanced Lignocellulosics (PALS) [grant number IH170100020] is gratefully acknowledged. We thank Matthieu Mention for his assistance in the synthesis of alkyne-modified DES and Ruth Melany Barajas for her assistance in the ICP-OES analysis. The authors acknowledge the use of the instruments and scientific and technical assistance of Tim Williams at the Monash Centre for Electron Microscopy, a Node of Microscopy Australia. We also thank Grand Reims and Région Grand Est for their financial support.

Appendix A. Supplementary data

Supplementary data to this article can be found online at <https://doi.org/10.1016/j.mtbio.2021.100126>.

References

- [1] A.L. Sobolewski, W. Domcke, Molecular mechanisms of the photostability of life, *Phys. Chem. Chem. Phys.* 12 (2010) 4897–4898, <https://doi.org/10.1039/C005130F>.
- [2] J. Orazio, S. Jarrett, A. Amaro-Ortiz, T. Scott, UV radiation and the skin, *Int. J. Mol. Sci.* 14 (2013) 12222–12248, <https://doi.org/10.3390/ijms140612222>.
- [3] Y. Ji, L. Cai, T. Zheng, H. Ye, X. Rong, J. Rao, Y. Lu, The mechanism of UVB irradiation induced-apoptosis in cataract, *Mol. Cell. Biochem.* 401 (2015) 87–95, <https://doi.org/10.1007/s11010-014-2294-x>.
- [4] A.Q. Khan, J.B. Travers, M.G. Kemp, Roles of UVA radiation and DNA damage responses in melanoma pathogenesis, *Environ. Mol. Mutagen.* 59 (2018) 438–460, <https://doi.org/10.1002/em.22176>.
- [5] Z.A. Lewicka, A.F. Benedetto, D.N. Benoit, W.W. Yu, J.D. Fortner, V.L. Colvin, The structure, composition, and dimensions of TiO₂ and ZnO nanomaterials in commercial sunscreens, *J. Nanoparticle Res.* 13 (2011) 3607, <https://doi.org/10.1007/s11051-011-0438-4>.
- [6] M.S. Latha, J. Martis, V. Shobha, R. Sham Shinde, S. Bangera, B. Krishnankutty, S. Bellary, S. Varughese, P. Rao, B.R. Naveen Kumar, Sunscreening agents: a review, *J. Clin. Aesthet. Dermatol.* 6 (2013) 16–26.
- [7] S.T. Butt, T. Christensen, Toxicity and phototoxicity of chemical sun filters, *Radiat. Protect. Dosim.* 91 (2000) 283–286, <https://doi.org/10.1093/oxfordjournals.rpd.a033219>.
- [8] L.T. Ngoc, V.V. Tran, J.Y. Moon, M. Chae, D. Park, Y.C. Lee, Recent trends of sunscreen cosmetic: an update review, *Cosmetics* 6 (2019), <https://doi.org/10.3390/cosmetics6040064>.
- [9] C. Milkowski, D. Strack, Sinapate esters in brassicaceous plants: biochemistry, molecular biology, evolution and metabolic engineering, *Planta* 232 (2010) 19–35, <https://doi.org/10.1007/s00425-010-1168-z>.
- [10] M.D. Horbury, E.L. Holt, L.M.M. Mouterde, P. Balaguer, J. Cebrian, L. Blasco, F. Allais, V.G. Stavros, Towards symmetry driven and nature inspired UV filter design, *Nat. Commun.* 10 (2019) 4748, <https://doi.org/10.1038/s41467-019-12719-z>.
- [11] A.L. Flourat, J. Combes, C. Bailly-Maitre-Grand, K. Magnien, A. Haudrechy, J.-H. Renault, F. Allais, Accessing p-hydroxycinnamic acids: chemical synthesis, biomass recovery, or engineered microbial production? *ChemSusChem* 14 (2021) 118–129, <https://doi.org/10.1002/cssc.202002141>.
- [12] C. Peyrot, M.M. Mention, F. Brunissen, F. Allais, Sinapic acid esters: octinoxate substitutes combining suitable UV protection and antioxidant activity, *Antioxidants* 9 (2020) 782, <https://doi.org/10.3390/antiox9090782>.

- [13] L.M.M. Mouterde, F. Allais, Microwave-assisted knoevenagel-dobner reaction: an efficient method for naturally occurring phenolic acids synthesis, *Front. Chem.* 6 (2018) 426, <https://doi.org/10.3389/fchem.2018.00426>.
- [14] D.J. Mendoza, L.M.M. Mouterde, C. Browne, V.S. Raghuvanshi, G.P. Simon, G. Garnier, F. Allais, Grafting nature-inspired and bio-based phenolic esters onto cellulose nanocrystals gives biomaterials with photostable Anti-UV properties, *ChemSusChem* 13 (2020) 6552–6561, <https://doi.org/10.1002/cssc.202002017>.
- [15] H.C. Kolb, M.G. Finn, K.B. Sharpless, Click chemistry: diverse chemical function from a few good reactions, *Angew. Chem. Int. Ed.* 40 (2001) 2004–2021, [https://doi.org/10.1002/1521-3773\(20010601\)40:11<2004::AID-ANIE2004>3.0.CO;2-5](https://doi.org/10.1002/1521-3773(20010601)40:11<2004::AID-ANIE2004>3.0.CO;2-5).
- [16] C.W. Tornøe, C. Christensen, M. Meldal, Peptidotriazoles on solid Phase: [1,2,3]-Triazoles by regioselective copper(I)-Catalyzed 1,3-dipolar cycloadditions of terminal alkynes to azides, *J. Org. Chem.* 67 (2002) 3057–3064, <https://doi.org/10.1021/jo011148j>.
- [17] D.J. Mendoza, C. Browne, V.S. Raghuvanshi, L.M.M. Mouterde, G.P. Simon, F. Allais, G. Garnier, Phenolic ester-decorated cellulose nanocrystals as UV-absorbing nanoreinforcements in polyvinyl alcohol films, *ACS Sustain. Chem. Eng.* 9 (2021) 6427–6437, <https://doi.org/10.1021/acssuschemeng.1c01148>.
- [18] D. Klemm, D. Schumann, F. Kramer, N. Heßler, D. Koth, B. Sultanova, Nanocellulose materials – different cellulose, different functionality, *Macromol. Symp.* 280 (2009) 60–71, <https://doi.org/10.1002/masy.200950608>.
- [19] D.J. Mendoza, C. Browne, V.S. Raghuvanshi, G.P. Simon, G. Garnier, One-shot TEMPO-periodate oxidation of native cellulose, *Carbohydr. Polym.* 226 (2019) 115292, <https://doi.org/10.1016/j.carbpol.2019.115292>.
- [20] D.J. Mendoza, L. Hossain, C. Browne, V.S. Raghuvanshi, G.P. Simon, G. Garnier, Controlling the transparency and rheology of nanocellulose gels with the extent of carboxylation, *Carbohydr. Polym.* 245 (2020) 116566, <https://doi.org/10.1016/j.carbpol.2020.116566>.
- [21] M. Irfan, B. Aneja, U. Yadava, S.I. Khan, N. Manzoor, C.G. Daniliuc, M. Abid, Synthesis, QSAR and anticandidal evaluation of 1,2,3-triazoles derived from naturally bioactive scaffolds, *Eur. J. Med. Chem.* 93 (2015) 246–254, <https://doi.org/10.1016/j.ejmech.2015.02.007>.
- [22] K. Missoum, M.N. Belgacem, J.-P. Barnes, M.-C. Brochier-Salon, J. Bras, Nanofibrillated cellulose surface grafting in ionic liquid, *Soft Matter* 8 (2012) 8338–8349, <https://doi.org/10.1039/c2sm25691f>.
- [23] S. Eyley, W. Thielemans, Surface modification of cellulose nanocrystals, *Nanoscale* 6 (2014) 7764–7779, <https://doi.org/10.1039/c4nr01756k>.
- [24] M. Maliha, R. Brammananth, J. Dyson, R.L. Coppel, M. Werrett, P.C. Andrews, W. Batchelor, Biocompatibility and selective antibacterial activity of a bismuth phosphinato-nanocellulose hydrogel, *Cellulose* 28 (2021) 4701–4718, <https://doi.org/10.1007/s10570-021-03835-5>.
- [25] R.M. Barajas-Ledesma, L. Hossain, V.N.L. Wong, A.F. Patti, G. Garnier, Effect of the counter-ion on nanocellulose hydrogels and their superabsorbent structure and properties, *J. Colloid Interface Sci.* 599 (2021) 140–148, <https://doi.org/10.1016/j.jcis.2021.04.065>.
- [26] Y. Qian, X. Qiu, S. Zhu, Lignin: a nature-inspired sun blocker for broad-spectrum sunscreens, *Green Chem.* 17 (2015) 320–324, <https://doi.org/10.1039/C4GC01333F>.
- [27] A. McKinlay, B. Diffey, in: W.F.B. Passchier, B.F. M (Eds.), *Human exposure to Ultraviolet Radiation: risks and Regulations in A Reference Action Spectrum for Ultraviolet Induced Erythema in Human Skin*, Elsevier Science Publishers Amsterdam, The Netherlands, 1987, pp. 83–87.
- [28] A.F. Reano, F. Pion, S. Domenek, P.-H. Ducrot, F. Allais, Chemo-enzymatic preparation and characterization of renewable oligomers with bisguaiacol moieties: promising sustainable antiradical/antioxidant additives, *Green Chem.* 18 (2016) 3334–3345, <https://doi.org/10.1039/C6GC00117C>.
- [29] J.B. Lambert, S. Gronert, H.F. Shurvell, D. Lightner, *Organic Structural Spectroscopy*, Pearson Prentice Hall, 2011.
- [30] L. Zhou, H. He, M.C. Li, S. Huang, C. Mei, Q. Wu, Grafting polycaprolactone diol onto cellulose nanocrystals via click chemistry: enhancing thermal stability and hydrophobic property, *Carbohydr. Polym.* 189 (2018) 331–341, <https://doi.org/10.1016/j.carbpol.2018.02.039>.
- [31] S.B. Kedare, R.P. Singh, Genesis and development of DPPH method of antioxidant assay, *J. Food Sci. Technol.* 48 (2011) 412–422, <https://doi.org/10.1007/s13197-011-0251-1>.
- [32] P. Criado, C. Fraschini, M. Jamshidian, S. Salmieri, A. Safrany, M. Lacroix, Gamma-irradiation of cellulose nanocrystals (CNCs): investigation of physicochemical and antioxidant properties, *Cellulose* 24 (2017) 2111–2124, <https://doi.org/10.1007/s10570-017-1241-x>.
- [33] ISO, *Biological Evaluation of Medical Devices-Part 5: Test for in Vitro Cytotoxicity*, vol. 34, International Standardization for Organization, Geneva, Switzerland, 2009.
- [34] Z. Zhang, B. Zhang, N. Grishkewich, R. Berry, K.C. Tam, Cinnamate-functionalized cellulose nanocrystals as UV-shielding nanofillers in sunscreen and transparent polymer films, *Adv. Sustain. Syst.* 3 (2019) 1800156, <https://doi.org/10.1002/advsu.201800156>.
- [35] D.R. Sambandan, D. Ratner, Sunscreens: an overview and update, *J. Am. Acad. Dermatol.* 64 (2011) 748–758, <https://doi.org/10.1016/j.jaad.2010.01.005>.
- [36] M.D. Horbury, L.A. Baker, N.D.N. Rodrigues, W.-D. Quan, V.G. Stavros, Photoisomerization of ethyl ferulate: a solution phase transient absorption study, *Chem. Phys. Lett.* 673 (2017) 62–67, <https://doi.org/10.1016/j.cplett.2017.02.004>.
- [37] M.N. Clifford, Diet-derived phenols in plasma and tissues and their implications for health, *Planta Med.* 70 (2004) 1103–1114, <https://doi.org/10.1055/s-2004-835835>.
- [38] C. Rice-Evans, N. Miller, G. Paganga, Antioxidant properties of phenolic compounds, *Trends Plant Sci.* 2 (1997) 152–159, [https://doi.org/10.1016/S1360-1385\(97\)01018-2](https://doi.org/10.1016/S1360-1385(97)01018-2).
- [39] E. Bendary, R.R. Francis, H.M.G. Ali, M.I. Sarwat, S. El Hady, Antioxidant and structure–activity relationships (SARs) of some phenolic and anilines compounds, *Ann. Agric. Sci.* 58 (2013) 173–181, <https://doi.org/10.1016/j.aos.2013.07.002>.
- [40] N.E. Gislason, B.L. Currie, A.L. Waterhouse, Novel antioxidant reactions of cinnamates in wine, *J. Agric. Food Chem.* 59 (2011) 6221–6226, <https://doi.org/10.1021/jf200115y>.
- [41] A.R. Nunes, Í.G.P. Vieira, D.B. Queiroz, A.L.A.B. Leal, S. Maia Morais, D.F. Muniz, J.T. Calixto-Junior, H.D.M. Coutinho, Use of flavonoids and cinnamates, the main photoprotectors with natural origin, *Adv. Pharmacol. Sci.* 2018 (2018) 5341487, <https://doi.org/10.1155/2018/5341487>.
- [42] B. Cao, Y. Zheng, T. Xi, C. Zhang, W. Song, K. Burugapalli, H. Yang, Y. Ma, Concentration-dependent cytotoxicity of copper ions on mouse fibroblasts in vitro: effects of copper ion release from TCu380A vs TCu220C intra-uterine devices, *Biomed. Microdevices* 14 (2012) 709–720, <https://doi.org/10.1007/s10544-012-9651-x>.
- [43] N.S. Aston, N. Watt, I.E. Morton, M.S. Tanner, G.S. Evans, Copper toxicity affects proliferation and viability of human hepatoma cells (HepG2 line), *Hum. Exp. Toxicol.* 19 (2000) 367–376, <https://doi.org/10.1191/096032700678815963>.
- [44] B. Cao, T. Xi, Y. Zheng, Release behavior of cupric ions for TCu380A and TCu220C IUDs, *Biomed. Mater.* 3 (2008), 044114, <https://doi.org/10.1088/1748-6041/3/4/044114>.
- [45] C.A. Grillo, M.A. Reigosa, M.A. Fernández Lorenzo de Mele, Does over-exposure to copper ions released from metallic copper induce cytotoxic and genotoxic effects on mammalian cells? *Contraception* 81 (2010) 343–349, <https://doi.org/10.1016/j.contraception.2009.12.003>.
- [46] C. Gianfranco, H.G. Lene, N. Eustachio, R. Paolo, L. Elisabetta Di, C. Riccardo, B. Lavjay, F. Caterina, Skin allergy to azole antifungal agents for systemic use: a review of the literature, *Recent Pat. Inflamm. Allergy Drug Discov.* 13 (2019) 144–157, <https://doi.org/10.2174/1872213X13666190919162414>.